Positioning Based on Noise-Limited Censored Path Loss Data

Aki Karttunen, Mikko Valkama, and Jukka Talvitie
Faculty of Information Technology and Communication Sciences
Tampere University
Tampere, Finland
{aki.karttunen, mikko.valkama, jukka.talvitie}@tuni.fi

***Abstract*—Positioning is considered one of the most important features and enabler of various novel industry verticals in future radio systems. Since path loss or received signal strength-based measurements are widely available and accessible in the majority of wireless standards, path loss-based positioning has an important role among other positioning technologies. Conventionally path loss-based positioning has two phases; i) fitting a path loss model to training data, if such training data is available, and ii) determining link distance estimates based on the path loss model and calculating the position estimate. However, in both phases, the maximum measurable path loss is limited by measurement noise. Such immeasurable samples are called censored path loss data and such noisy data is commonly neglected in both the model fitting and in the positioning phase. In the case of censored path loss, the loss is known to be above a known threshold level and that *information* can be used in model fitting as well as in the positioning phase. In this paper, we examine and propose how to use censored path loss data in path loss model-based positioning and demonstrate with simulations the potential of the proposed approach for considerable improvements (over 30%) in positioning accuracy.**

***Index Terms*—positioning, path loss, path loss model, maximum-likelihood estimation, censored data, localization, shadow fading, wireless networks, probabilistic modeling.**

I. Introduction

Radio based positioning has rapidly grown into one of the most significant features in future wireless networks. As stated in the specifications of the upcoming 5^{th} generation new radio networks in [1], positioning has been considered as part of basic network capability, and it offers a wide variety of performance requirements tailored to specific needs of numerous use cases and industry verticals. Path loss (PL) or received signal strength-based positioning, studied earlier, for example, in [2]–[4], enables low-cost positioning capability especially for use cases with limited power and computational resources. In addition, path loss based positioning can introduce additional support to various other high-precision positioning and tracking solutions for increased positioning accuracy, availability, stability or reliability, as shown, for example, in [4]. Since path loss and received signal strength are power-related measurements, they are typically continually measured and monitored in mobile networks over multiple base stations (BS) to support mobility management and other radio resource management functionalities. Thus, path loss based positioning can rely on regular reference signals of the underlying communications system without introducing any additional training overhead due to positioning capability. However, due to challenging and highly dynamic propagation environment, PL-based positioning methods are typically limited to positioning accuracy of tens or hundreds of meters in outdoor cellular networks [2], [5].

Conventionally path loss based positioning has two phases; i) fitting a path loss model to training data, if such training data is available, and ii) determining link distance estimates based on the path loss model and calculating the position estimate. Channel measurements can be used to measure the training data and then a PL model can be fitted to the data [6]–[8]. The PL model describes the link distance dependency and the variation from the expected value, i.e., shadow fading (SF). Sometimes training data may be unavailable and the PL model can be taken from a standard channel model, e.g., [9]. Since PL is strongly distance-dependent, it can be used in positioning, and the probability distribution of the link distance estimate can be determined from the measured PL and the assumed PL model. In principle, distance estimates to three or more sources can give a unique position estimate.

The position estimate has several factors affecting the positioning accuracy. Shadow fading (SF) can be quite large in many environments [6]–[9]. Large SF leads to a large variance in the distance estimates which in turn negatively affects the accuracy. The number of the reference locations, i.e., BSs, the system geometry, as well as the BS antenna orientations are all important factors for the positioning accuracy. Naturally, many distance estimates give better accuracy than only a few. A third error source that we would like to point out is a possible difference in the PL model used in the positioning and the true PL behavior in the given environment. Such discrepancy can be due to unavailable training data, as mentioned before, or, e.g., outdated training data. Erroneous PL model will underestimate or overestimate the distance estimates leading to increased positioning errors.

In practice, the maximum measurable path loss is limited by measurement noise. Therefore, in both the training data and in the positioning it may happen that the PL value can not

The research leading to these results received funding from Academy of Finland project 323244 (LOCALCOM) and 328214 (ULTRA).

be determined. In that case, the PL is known to be more than the noise threshold level. When data above or below a certain range are immeasurable, meaning that all data above or below a certain range are counted, but not measured, it is called *censored* data [6], [7], [10]–[13]. The path loss model can be fitted to censored data by using Tobit maximum likelihood estimation (MLE) [6], [7]. Censored PL samples are typically ignored as outage and not taken into account which can lead to significant error in the PL model distribution. For example, in [6] it is shown by using measured path loss data that by ignoring the censored samples the slope of the PL model, i.e., path loss exponent, is drastically underestimated at 1.3 instead of 2.2. Thus it is important to use the Tobit MLE when fitting the model to the training data. Note that ignoring the censored PL data in the training phase may lead to a similarly erroneous PL model as when getting the model from literature without conducting the laborious training measurements.

Just as in the training phase, the noise threshold limits the maximum PL in the positioning phase. When PL measured from a certain BS is larger than the noise threshold, the true location is likely to be far from the BS, and the true distance is subject to the distance dependence of the PL and the threshold level. Therefore, measuring PL at the positioning phase is censored data in the same fashion as in the case of the training data. In the training data, there are two types of data samples; ones with measured PL and those with PL larger than the threshold. In the positioning phase, there are two types of data samples; ones with distance estimates and ones with distance estimates more than a threshold distance. In [14], [15], the likelihood of connecting or not connecting to a BS is taken into account in case of time-of-arrival positioning. In this paper, we frame this as Tobit MLE.

The censored PL data (may) exist in both in the training phase and the positioning phase. Therefore, in terms of taking or not taking in to account the censored samples, there are four options. In [6], fitting without the censored data is called ordinary least squares fitting (OLS) as opposed to the Tobit MLE. Similarly, for the positioning there is the ordinary positioning, using only the distance estimates from the contacted BSs, that we now call ordinary trilateration positioning (OTP), and there is the option to include the censored data with Tobit MLE. The four options are:

1) OLS-OPT, with ordinary least squares fitting to the training data and the ordinary trilateration positioning.
2) MLE-OPT, with Tobit MLE fitting to the training data and the ordinary trilateration positioning.
3) OLS-MLE, with ordinary least squares fitting to the training data and the Tobit MLE positioning.
4) MLE-MLE, with Tobit MLE fitting to the training data and the Tobit MLE positioning.

To the best of the authors' knowledge, this is the first time the noise-limited censored path loss data is considered in both phases of the PL model-based positioning. We will examine the influence of including the censored data through simple simulations with a typical log-distance PL model and illustrate the potential of the proposed approach for considerable improvements in positioning accuracy.

The remainder of the paper is organized as follows: Section II lists the path loss and antenna models used in this study. In Section III, the PL model is fitted to simulated training data. Positioning with or without the censored PL is examined in Section IV and the simulation results are presented in Section V. Finally, conclusions are given in Section VI.

II. Path Loss and Antenna Model

Path loss is the inverse of small-scale-averaged path gain between the base station (BS) and the mobile station (MS) calculated as the instantaneous local channel gain averaged over the small-scale fading. Typical PL model describes the statistical behavior of the PL assuming omni-directional antennas and includes equations for expected PL and the variations from the mean value-line, i.e., the shadow fading.

A simple log-distance path loss model is assumed as follows:

$$PL(d) = \overline{PL}(d) + S, \tag{1}$$

$$\overline{PL}(d) = 10 \cdot \alpha \cdot \log_{10}(d/\mathrm{d}_0) + \beta, \tag{2}$$

where S is the zero-mean shadow fading with variance σ^2, $\overline{PL}(d)$ is the link distance dependent expected path loss, and $\mathrm{d}_0 = 1$ m is a reference distance. Eq. (2) has two free parameters: path loss exponent α and floating intercept point β, which can be interpreted as the mean PL at d_0. Parameters α, β, and σ can be attained by fitting the model to measurement data or, e.g., taken from a channel model [9].

In this work, the parameter values are selected as approximate median values given in 3GPP model [9] for various environments including both line-of-sight (LOS) and non-line-of-sight (NLOS) in both outdoor and indoor environments. For simplicity we do not distinguish between LOS and NLOS nor do we specify the used radio frequency. We assume that the PL statistics are stationary and use the same PL model for all BSs [8], [16], [17]. The used parameters are $\alpha = 4$, $\beta = 60$ dB, and $\sigma = 7$ dB.

In case of a directive antenna, we approximate

$$PL(d, \theta) = PL(d) - G(\theta), \tag{3}$$

$$PL(d, \theta) = 10 \cdot \alpha \cdot \log_{10}(d/\mathrm{d}_0) + \beta - G(\theta) + S, \tag{4}$$

where $G(\theta)$ is the antenna gain pattern. Simple BS antenna pattern from [9] [18] is used:

$$A(\theta) = -\min(12(\theta/\theta_{3\mathrm{dB}})^2, 20\mathrm{dB}), \tag{5}$$

where $\min(\cdot)$ denotes the minimum function, θ is the offset angle from boresight, and $\theta_{3\mathrm{dB}}$ is the antenna half-power beam-width. The relative sidelobe level is fixed at a constant 20 dB below the maximum gain. Antenna gain $G(\theta)$ is the $A(\theta)$ normalized for unit gain, i.e., for same total radiated power as omni-directional antenna with $G(\theta) = 0$ dB. The BS is assumed to cover 360° with N antenna beams with 3 dB beam overlap, i.e., $\theta_{3\mathrm{dB}} = 360°/N$. The omni-directional and examples of directive antenna patterns are illustrated in

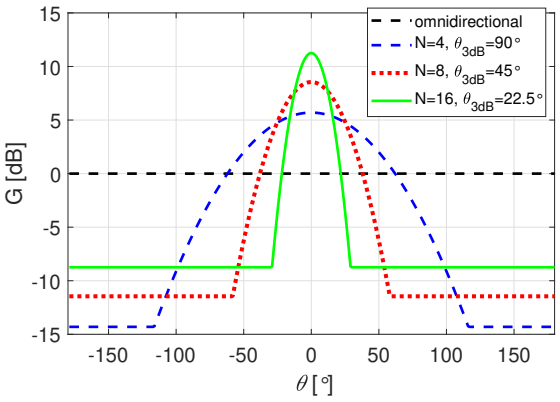

Fig. 1. Antenna gain as a function of the offset angle θ. The directive beam patterns have beam-width of $\theta_{3\text{dB}} = 360°/N$.

Fig. 1. Only the omni-directional and 8-sector BS antennas ($N = 8$, $\theta_{3\text{dB}} = 45°$, $\max(G) = 9$ dB) are taken as examples in this paper. The MS has omni-directional antenna. The approximation (3) assumes that (most of) the power is near the direct line between BS and MS. More accurately, the antenna gain is applied to the multipaths that may arrive/depart at any angle [9]. Nevertheless, the simplistic approximation is assumed as it allows simple simulations with directive antennas.

The noise threshold level PL^* limits the maximum path loss that can be measured. In this work, we set the noise threshold at 140 dB. The expected PL (2) reaches the 140-dB level at link distance of 100 m with $\alpha = 4$ and $\beta = 60$ dB and omni-directional antennas. Therefore, PL at that distance has a 50% probability of being immeasurable, i.e., censored. Due to the large shadow fading $\sigma = 7$ dB there is significant probability of censored PL between 40 m to 220 m ($\overline{PL}(d) \pm 1.96\sigma$). With a directive antenna, the positive gain pushes these distances further away from the BS.

Shadow fading inter-site cross-correlation is small for widely spaced sites and large for closely spaced base stations [19], [20]. Therefore we use zero correlation between BS sites and same SF for different beams of the same BS location. In this work, we do not use any tracking algorithm, and therefore SF auto-correlation function and correlation distance are not defined.

In summary, we assume the log-distance PL model (4) with $\alpha = 4$, $\beta = 60$ dB, $\sigma = 7$ dB, and noise threshold at 140 dB. The BS antenna is either omni-directional or eight-sector directive antenna that covers the 360° with $\theta_{3\text{dB}} = 45°$ and $\max(G) = 9$ dB.

III. Censored Path Loss and Model Fitting

The first phase of PL model-based positioning is the measurement of training data and fitting the model to the data. The purpose of the training phase is to get a PL model that accurately describes the PL probability distribution that can be then used in the positioning phase.

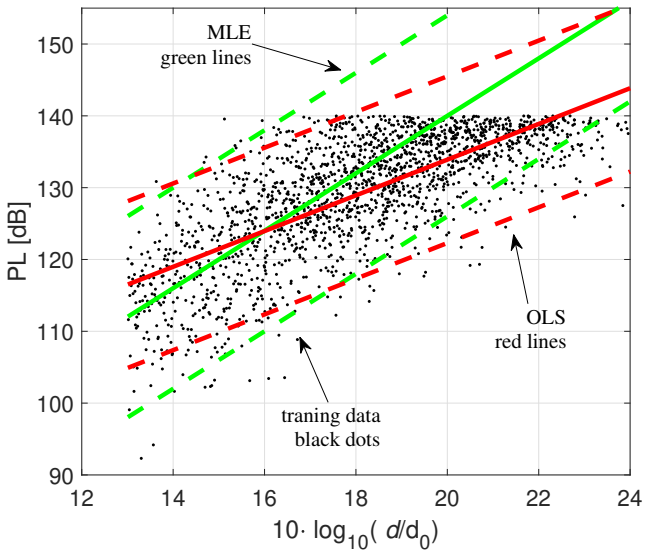

Fig. 2. Fitting the path loss model to the training data with OLS (green) and MLE (red). Training data with PL under the noise threshold is shown with black dots, solid lines show $\overline{PL}(d)$ and the dash lines are $\overline{PL}(d) \pm 1.96\hat{\sigma}$.

Training data is created with (1)-(2) and illustrated in Fig. 2. The noise threshold is 140 dB. Data is created with a uniform distribution of distances between 20 m and 500 m with a large sample size to avoid uncertainty in the parameter estimates [2], [6]. The PL model can be fitted to the data using OLS or Tobit MLE [6]. With OLS the noise-limited censored data is ignored and with MLE all data are taken into account.

The likelihood of measuring PL is [6]

$$l(PL) = (1/\sigma)\phi((PL - \overline{PL})/\sigma), \tag{6}$$

where σ is the standard deviation (std) of the shadow fading, and $\overline{PL}$ is the path loss model. Here, $\phi(\cdot)$ is the standard normal probability density function (PDF). The log-likelihood function for known PL samples at distances d_i is

$$LLF = \sum_{i=1}^{N_s} \left(-\ln\sigma + \ln\phi\left(\frac{PL(d_i) - \overline{PL}(d_i)}{\sigma}\right)\right), \tag{7}$$

where N_s is the number of uncensored data samples.

The likelihood of measuring $PL > PL^*$ is [6]

$$l(PL > PL^*) = 1 - \Phi((PL^* - \overline{PL})/\sigma), \tag{8}$$

where the path loss level for the noise threshold is PL^*, and $\Phi(\cdot)$ is the cumulative distribution function (CDF) of the standard normal distribution. The log-likelihood function for censored samples at distances d_i is

$$LLF^* = \sum_{i=1}^{N_s^*} \ln\left(1 - \Phi\left(\frac{PL^* - \overline{PL}(d_i)}{\sigma}\right)\right), \tag{9}$$

where * refers to censored data, i.e., N_s^* is the number of censored data points. The path loss parameters are then

estimated as the minimum of the negative of the log-likelihood function as

$$[\hat{\alpha}, \hat{\beta}, \hat{\sigma}] = \arg\min_{\alpha,\beta,\sigma} \{-(LLF + LLF^*)\}. \quad (10)$$

The fitted PL models are illustrated in Fig. 2. The OLS fitting gives parameter estimates $\hat{\alpha} \approx 2.5$, $\hat{\beta} \approx 83$ dB, and $\hat{\sigma} \approx 5.7$ dB. The MLE gives parameter estimates $\hat{\alpha} \approx 4$, $\hat{\beta} \approx 60$ dB, and $\hat{\sigma} \approx 7$ dB. The MLE estimated are very close to the true values $\alpha = 4$, $\beta = 60$ dB, and $\sigma = 7$ dB. As can be seen, ignoring the censored samples can lead to significant errors in the PL model distribution. The same conclusion is made in [6], [7], and in this paper, we will study the effects on positioning accuracy.

In principle, path loss-based positioning can be done without the training phase. In that case, the PL-model parameters can be taken, e.g., from a standard channel model. The OLS fitting result can be seen as serving double duty, both as the OLS fitting result and as the (rather poor) educated guess in the absence of training data.

IV. Censored Path Loss and Positioning

Path loss model-based positioning is based on getting distance estimates from measured PL to BSs with known locations. For a given distance the PL model describes a probability distribution for PL or inversely a PL value gives a distribution for the link distance. The width of the distribution is proportional to shadow fading. In ordinary trilateration positioning (OTP), distance estimates to BSs are used to trilaterate the positioning estimate.

When fitting the model to training data the censored PL is a measurement result at a known link distance and PL known to be more than the noise threshold level. In positioning, censored PL is an uncontacted BS due to PL larger than the threshold. Therefore, the minimum link distance has a probability distribution associated with the noise threshold level. Thus, failing to contact a given BS has *position information* as it means that the true position is unlikely to be close to that particular BS. Next, we will frame the positioning problem as a Tobit maximum likelihood estimation (MLE) in a similar manner as (7)-(10).

Let us first write the log-distance as $q = 10 \cdot \log_{10}(d/d_0)$ then the expected distance is

$$\overline{q}(PL_i, \theta_i) = (PL_i - \beta + G(\theta_i))/\alpha, \quad (11)$$

$$q^*(\theta_i) = (PL^* - \beta + G(\theta_i))/\alpha, \quad (12)$$

where PL_i is the measured PL, PL^* is the noise threshold, q^* is the corresponding log-distance, and the standard deviation corresponding to shadow fading is σ/α. q_i is the log-distance from point (x, y) to BS$_i$ (or beam) and θ_i is the beam offset angle.

The log-likelihood function for known measured PL at point (x, y) is

$$LLF = \sum_{i=1}^{N_{BS}} \left(-\ln \frac{\sigma}{\alpha} + \ln \phi \left(\frac{q_i - \overline{q}(PL_i, \theta_i)}{\sigma/\alpha} \right) \right), \quad (13)$$

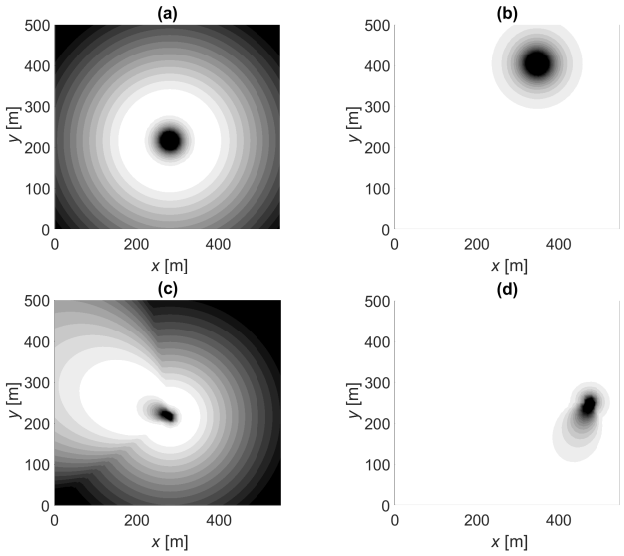

Fig. 3. Likelihood function illustrations: (a) measured PL and omnidirectional antenna, (b) censored PL and omnidirectional antenna, (c) measured PL and directive beam ($N = 8$), (d) censored PL and directive beam ($N = 8$). White is likely, gray is possible, and black is unlikely location.

where N_{BS} is the number of BSs (or directive beams) with measured PL under the noise threshold. The log-likelihood function for censored PL at point (x, y) is

$$LLF^* = \sum_{i=1}^{N^*_{BS}} \ln \left(1 - \Phi \left(\frac{q^*(\theta_i) - q_i}{\sigma/\alpha} \right) \right), \quad (14)$$

where N^*_{BS} is the number of BSs (or directive beams) with censored PL. The position estimate $(\hat{x}, \hat{y})$ is derived as the minimum of the negative of the log-likelihood function as

$$[\hat{x}, \hat{y}] = \operatorname*{argmin}_{x,y} \{-(LLF + LLF^*)\}. \quad (15)$$

In this work, OTP uses only (13) and (15) and the MLE positioning uses (13)-(15). Thus the only difference is whether or not the location information from the noise-limited censored PL data is used.

Likelihood function illustrations are presented in Fig. 3. In Fig. 3 (a) is the LLF_i of a contacted BS with an omnidirectional antenna where the highest likelihood is found on a ring around the BS. In Fig. 3 (b) is the LLF^*_i of an uncontacted BS showing a low likelihood close to the BS. Fig. 3 (c) and (d) are the corresponding examples with a directive antenna where the likelihood functions are stretched by the antenna gain pattern. Fig. 4 shows an example of the sum of the likelihood functions in one location using the four options. In this example, the distance between BSs is 248 m, BSs antennas with eight beams ($N = 8$, $\theta_{3\text{dB}} = 45°$), and three BSs are contacted with a total of four beams ($PL < PL^*$). The positioning errors are 81 m, 72 m, 9 m, and 14 m for OLS-OTP, MLE-OTP, OLS-MLE, and MLE-MLE, respectively. Using MLE positioning results in smaller and narrower likelihood function optimum.

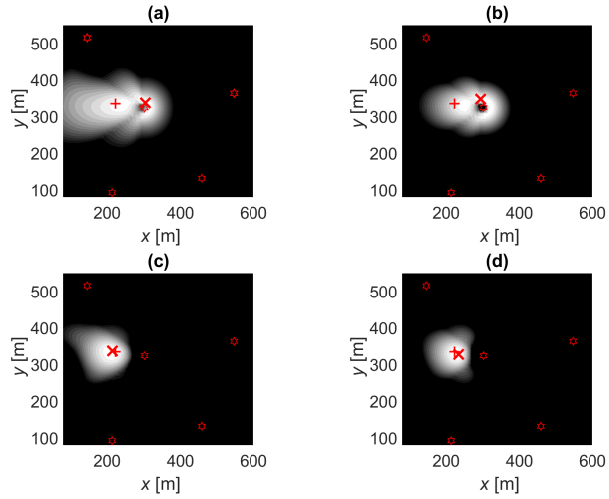

Fig. 4. Likelihood function illustrations: true location (+), position estimate (x), BSs (stars), contact to three BSs with directive antennas ($N = 8$) at $(x_{\mathrm{BS}}, y_{\mathrm{BS}}) = (302, 324)$, $(547, 363)$, and $(146, 516)$. White is likely, gray is possible, and black is unlikely location.
(a) OLS-OPT: ordinary least squares fitting and trilateration positioning.
(b) MLE-OPT: Tobit MLE fitting and the ordinary trilateration positioning.
(c) OLS-MLE: ordinary least squares fitting and the Tobit MLE positioning.
(d) MLE-MLE: Tobit MLE fitting and the Tobit MLE positioning.

V. Simulations

The four options with and without the censored data are compared by conducting simulations in a regular BS grid, following hexagonal layout. The true PL values are calculated based on (4) with parameters $\alpha = 4$, $\beta = 60$ dB, and $\sigma = 7$ dB. The positioning is based on PL model derived, in Section III, either by OLS ($\alpha \approx 2.5$, $\beta \approx 83$ dB, and $\sigma \approx 5.7$ dB) or by MLE ($\alpha = 4$, $\beta = 60$ dB, and $\sigma = 7$ dB). Positioning is done either with OTP or with Tobit MLE, as presented in Section IV. Therefore, the four options are OLS-OTP, MLE-OTP, OLS-MLE, and MLE-MLE.

Positioning error is the distance between the true position and the estimated position. Results are presented in Figs. 5 - 6 and Tables I - II. These statistics are based on 10000 samples with random true location and different realizations of SF.

The BS grid density affects the positioning accuracy. In a regular hexagonal grid, the distance between BSs is constant. Three BS grid densities are considered leading to an average of 2, 3, or 5 contacted BSs. Each average number of contacted BSs $\overline{BS}$ corresponds to a constant distance between neighbours d_{BS}. Two BS antennas are considered, omni-directional and directional beams with $N = 8$ and $\theta_{3\mathrm{dB}} = 45°$.

In all of the simulated cases, OLS-OTP is the worst. It is the worst-case scenario with the PL model that does not fit the reality and positioning that does not use all the available information. For example, with omni-directional antennas and $\overline{BS} = 2$, the median errror is 58 m, 43 m, 46 m, and 31 m with OLS-OTP, MLE-OTP, OLS-MLE, and MLE-MLE, respectively. In this case, there is a 47% improvement from OLS-OTP to MLE-MLE. The positioning error with the directive antennas is smaller than with the omni-directional antennas

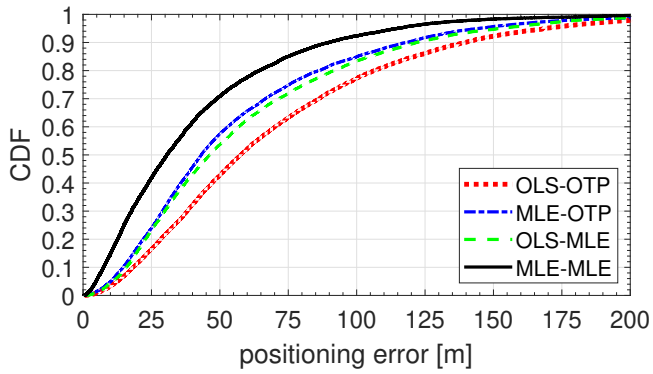

Fig. 5. CDF of positioning error. Model fitting to training data with ordinary least squares (OLS-) or Tobit MLE fitting (MLE-) and positioning with either ordinary trilateration (-OTP) of Tobit MLE positioning (-MLE). Base stations have eight beams with $\theta_{3\mathrm{dB}} = 45°$ and the average number of contacted BSs is 2.

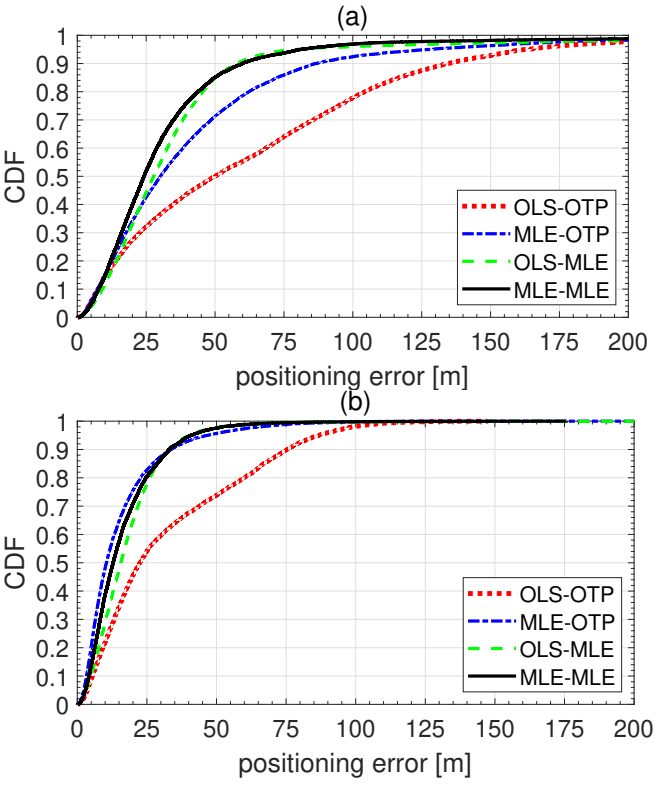

Fig. 6. CDF of positioning error. Model fitting to training data with ordinary least squares (OLS-) or Tobit MLE fitting (MLE-) and positioning with either ordinary trilateration (-OTP) of Tobit MLE positioning (-MLE). Base stations have omni-directional antennas and the average number of contacted BSs is 2 (a) and 5 (b).

and, similarly, with the denser BS grid the errors are smaller. These trends apply to all the presented cases.

Using MLE in either phase improves accuracy. The best example of this is a dense BS grid with $\overline{BS} = 5$ and the directive antennas resulting in the 90% percentile error of 75 m with OLS-OTP and a 55% improvement to about 33 m with MLE in either or both phases (see Table II). Using the noise-

TABLE I

POSITIONING ERROR 50% AND 90% PERCENTILES. BASE STATIONS HAVE OMNI-DIRECTIONAL ANTENNAS AND THE AVERAGE NUMBER OF CONTACTED BSS IS 2, 3, OR 5.

$\overline{BS}$	2		3		5	
d_{BS}	158		130		100	
	50%	90%	50%	90%	50%	90%
OLS-OTP	58	140	47	105	32	76
MLE-OTP	43	118	31	72	22	49
OLS-MLE	46	122	31	74	21	47
MLE-MLE	31	90	30	72	21	45

TABLE II

POSITIONING ERROR 50% AND 90% PERCENTILES. BASE STATIONS HAVE EIGHT BEAMS WITH $\theta_{3\mathrm{dB}} = 45^\circ$ AND THE AVERAGE NUMBER OF CONTACTED BSS IS 2, 3, OR 5.

$\overline{BS}$	2		3		5	
d_{BS}	248		201		155	
	50%	90%	50%	90%	50%	90%
OLS-OTP	50	135	43	101	22	75
MLE-OTP	30	87	22	64	10	34
OLS-MLE	28	58	18	43	16	33
MLE-MLE	24	60	18	42	13	33

limited censored PL with MLE in both phases, MLE-MLE, is, in general, the most accurate option.

Lastly, let us compare MLE-OTP to OLS-MLE. The median and the 90% percentiles are very close to each other. In MLE-OTP, the positioning is based on the correct PL model but the censored PL is not used in the positioning phase. In OLS-MLE, the censored PL is used in the positioning phase with MLE but the OLS fitting results in wrong parameter estimates, as shown in Section III. As pointed out earlier, the OLS fitting result can be also interpreted as (a rather poor) educated guess in the absence of training data. Using MLE in the positioning phase compensates for the poor PL model. Therefore, it can be concluded that, if the noise-limited censored PL is taken in to account in the positioning phase, the training phase is perhaps not needed.

VI. CONCLUSIONS AND FUTURE WORK

In this paper, we have shown that the noise-limited censored PL data can be used in the training and positioning phases of PL model-based positioning. The censored data, i.e., when PL is larger than the noise threshold, can be taken into account using Tobit MLE when fitting the model to the training data and also in the positioning phase.

Simulations are conducted with a simple log-distance law PL model that shows improved positioning accuracy when the censored PL is properly taken in to account with MLE. Results also indicate that, if the censored PL is taken into account in the positioning phase, then the accuracy of the PL model fitting to training data becomes far less important. This suggests that training data might not be needed assuming the log-distance law PL model is a good approximation of realistic path loss.

Future work on this topic should include realistic PL data, the selection criterion for which BSs are included, and the inclusion of a tracking algorithm.

REFERENCES

[1] 3GPP, "Service requirements for the 5G system," *3GPP TS 22.261 V17.1.0 (2019-12)*.

[2] H. Nurminen, J. Talvitie, S. Ali-Löytty, P. Müller, E.-S. Lohan, R. Piché, and M. Renfors, "Statistical path loss parameter estimation and positioning using RSS measurements in indoor wireless networks," in *2012 International Conference on Indoor Positioning and Indoor Navigation (IPIN)*, Nov. 2012.

[3] C. Luo, S. I. McClean, G. Parr, L. Teacy, and R. De Nardi, "UAV position estimation and collision avoidance using the extended kalman filter," *IEEE Transactions on Vehicular Technology*, vol. 62, no. 6, pp. 2749–2762, July 2013.

[4] H. Xiong, M. Peng, S. Gong, and Z. Du, "A novel hybrid RSS and TOA positioning algorithm for multi-objective cooperative wireless sensor networks," *IEEE Sensors Journal*, vol. 18, no. 22, pp. 9343–9351, Nov. 2018.

[5] S. Mazuelas, F. A. Lago, D. González, A. Bahillo, J. Blas, P. Fernández, R. M. Lorenzo, and E. J. Abril, "Dynamic estimation of optimum path loss model in a RSS positioning system," in *2008 IEEE/ION Position, Location and Navigation Symposium*, May 2008, pp. 679–684.

[6] C. Gustafson, T. Abbas, D. Bolin, and F. Tufvesson, "Statistical modeling and estimation of censored pathloss data," *IEEE Wireless Commun. Lett.*, vol. 4, no. 5, pp. 569–572, Oct. 2015.

[7] A. Karttunen, C. Gustafson, A. F. Molisch, R. Wang, S. Hur, J. Zhang, and J. Park, "Path loss models with distance-dependent weighted fitting and estimation of censored path loss data," *IET Microwaves, Antennas Propagation*, vol. 10, no. 14, pp. 1467–1474, Nov. 2016.

[8] K. Haneda, N. Omaki, T. Imai, L. Raschkowski, M. Peter, and A. Roivainen, "Frequency-agile pathloss models for urban street canyons," *IEEE Transactions on Antennas and Propagation*, vol. 64, no. 5, pp. 1941–1951, 2016.

[9] 3GPP, "Study on channel model for frequencies from 0.5 to 100 GHz," *3GPP TR 38.901 V14.3.0 (2018-01)*.

[10] J. Tobin, "Estimation of relationships for limited dependent variables," *Econometrica*, vol. 26, no. 1, pp. 24–36, Jan. 1958.

[11] H. O. Hartley, "Maximum likelihood estimation from incomplete data," *Biometrics*, vol. 14, no. 2, pp. 174–194, 1958.

[12] A. P. Dempster, N. M. Laird, and D. B. Rubin, "Maximum likelihood from incomplete data via the EM algorithm," *Journal of the royal statistical society. Series B (methodological)*, pp. 1–38, 1977.

[13] A. Karttunen, J. Järveläinen, S. L. H. Nguyen, and K. Haneda, "Modeling the multipath cross-polarization ratio for 5–80-GHz radio links," *IEEE Transactions on Wireless Communications*, vol. 18, no. 10, pp. 4768–4778, Nov. 2019.

[14] S. G. Nagarajan, P. Zhang, and I. Nevat, "Geo-spatial location estimation for internet of things (IoT) networks with one-way time-of-arrival via stochastic censoring," *IEEE Internet of Things Journal*, vol. 4, no. 1, pp. 205–214, Feb. 2017.

[15] I. Nevat, F. Septier, K. Avnit, G. W. Peters, and L. Clavier, "Joint localization and clock offset estimation via time-of-arrival with ranging offset," in *2018 26th European Signal Processing Conference (EUSIPCO)*, Sep. 2018, pp. 672–676.

[16] A. Karttunen, A. F. Molisch, S. Hur, J. Park, and C. J. Zhang, "Spatially consistent street-by-street path loss model for 28-GHz channels in micro cell urban environments," *IEEE Transactions on Wireless Communications*, vol. 16, no. 11, pp. 7538–7550, Nov. 2017.

[17] V. Erceg, L. J. Greenstein, S. Y. Tjandra, S. R. Parkoff, A. Gupta, B. Kulic, A. A. Julius, and R. Bianchi, "An empirically based path loss model for wireless channels in suburban environments," *IEEE Journal on selected areas in communications*, vol. 17, no. 7, pp. 1205–1211, July 1999.

[18] "ITU-R M. 2135-1: Guidelines for evaluation of radio interface technologies for IMT-Advanced," Technical report, ITU, Tech. Rep., 2009.

[19] N. Jaldén, P. Zetterberg, B. Ottersten, and L. Garcia, "Inter-and intrasite correlations of large-scale parameters from macrocellular measurements at 1800 mhz," *EURASIP Journal on Wireless Communications and Networking*, vol. 2007, pp. 1–12, 2007.

[20] K. Zayana and B. Guisnet, "Measurements and modelisation of shadowing cross-correlations between two base-stations," in *ICUPC '98. IEEE 1998 International Conference on Universal Personal Communications. Conference Proceedings (Cat. No.98TH8384)*, vol. 1, Oct. 1998, pp. 101–105 vol.1.